Proceedings of the Sixteenth International Conference on
Computational Structures Technology
Edited by: P. Iványi, J. Kruis and B.H.V. Topping
Civil-Comp Conferences, Volume 14, Paper 3.2
Civil-Comp Press, Edinburgh, United Kingdom, 2026
ISSN: 2753-3239, doi: 10.4203/ccc.14.3.2

Virtual Element Method for Topology Optimization of Contact Problems

A. Myśliński

Systems Research Institute, Warszawa, Polska

Abstract

This paper is concerned with the application of the virtual element method (VEM) to solve topology optimization problems for two-dimensional structures in contact. The goal is to design an optimal layout for two bodies in bilateral frictional elasto-plastic contact to minimize the maximal contact stress along the joint boundary of the bodies and to ensure the uniform distribution of this stress. This work is concerned with the extension of the VEM to nonlinear problems. The key feature distinguishing VEM from the classical finite element method is that the local basis functions in VEM are only implicitly known. VEM is used to approximate the governing boundary value problem as well as the gradient flow equation exploiting the calculated derivative of the cost functional. Generalized Newton method is used to solve numerically this discretized optimization problem. Numerical examples are provided and discussed.

Keywords: topology optimization, contact problem, friction, elasto-plastic material, virtual element method, gradient flow equation.

1 Introduction

Topology optimization consists in material distribution within the design domain to minimize the given cost functionals describing required features of the structure [2, 14, 15]. Most research related to topology optimization has been concerned with linear elastic structures (see references in [2]). The amount of papers dealing with nonlinear elastic structures or nonlinear mechanical behavior is limited. The ability to take into account elasto-plastic materials is of great interest of industrial engineers. Plasticity models account for irreversible microscopic mechanical defects resulting in plastic areas which tend to deform more than elastic ones. This may lead either to wear and fatigue of the structure or to its damage. The fundamentals of the theory of plasticity and elasto-plasticity, including both mechanical and mathematical aspects, are presented and discussed in many monographs (see references in [9]). The contact problems between elasto-plastic bodies governed by variational inequalities are discussed in [6, 8, 14]. Shape or topology optimization of elasto-plastic structures have been investigated in [2, 14, 15].

The Virtual Element Method (VEM) [4] is a numerical technique designed for polytopal discretization. Its mathematical foundations have been well established [4, 5, 7, 10, 12, 16, 17, 21] and its benefits have been explored on numerous applications. Inspired by the ideas put forward by the Mimetic Finite Difference method [13] VEM was devised and put into a Galerkin framework [13], ultimately becoming a generalization of standard FEM that allows using arbitrary polytopal meshes. The main idea behind VEM is that the local shape function space in each element is defined implicitly - thus the name virtual. Furthermore, shape functions are constructed according to an integer k, which represents the interpolation order of the approximation. In spite of its short life span, VEM has already caught the attention of the computational mechanics community (see references in [18, 19]). The method was designed to handle arbitrarily shaped polytopal discretization, which are particularly convenient for meshing complex geometries. This endows VEM with unmatched flexibility in the pre-processing stage of the analysis.

The aim of this work is to solve numerically the shape and/or topology optimization problem for two bodies in contact assuming static elasto-plastic rather than elastic material model. The optimization problem consists in finding such shape of the domain occupied by the body in contact to minimize the stress along the contact boundary. The bilateral elasto-plastic contact problem with Tresca friction is formulated using the small strain plasticity material model [6]. This problem is reformulated as dual variational problem where the displacement and the generalized stress of the body are governed by the system of two coupled variational inequalities. Using Moreau–Yosida as well as friction regularization techniques [15] these inequalities are transformed into the set of two coupled nonlinear equations. The topology optimization problem for the bodies in contact is formulated in terms of material density function. The derivative of the cost functional is calculated and gradient flow equation formulated. The optimization problem is discretized using the virtual finite element method. The semi-smooth Newton method is used to solve the discrete contact problem. Numerical

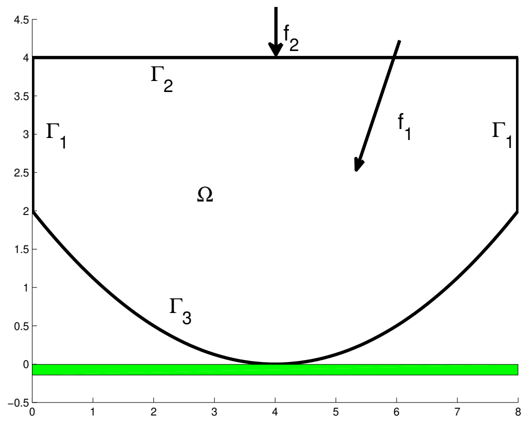

Figure 1: Contact problem.

results are reported and discussed.

2 Topology optimization problem

Topology optimization consists in material distribution within the design domain to minimize the given cost functionals describing required features of the structure [3, 10]. Topology optimization of contact problems aims to reduce maximal contact stress generating wear or fatigue of the contacting surfaces.

2.1 Contact problem

Consider a body occupying a bounded domain $\Omega \subset R^d$, $d = 2, 3$, with a Lipschitz continuous boundary Γ (see Fig. 1). The boundary Γ is divided into three open disjoint and measurable parts Γ_1, Γ_2 and Γ_3 such that $meas(\Gamma_1) > 0$. The displacement of the body subject to deformation by a given volume force of density $f_1 = f_1(x)$, $x \in \Omega$, and a surface traction of density $f_2 = f_2(x)$ applied on the boundary Γ_2 is denoted by $u = \{u_i\}_{i=1}^d$. The body is clamped along the boundary Γ_1, i.e., its displacement vanishes there. Along the boundary Γ_3 the body is assumed to be in bilateral frictional contact with the rigid foundation. The friction phenomenon is modeled by Tresca's law. The forces f_1 and f_2 are acting slow enough to neglect the inertial terms. The domain Ω is filled with a material undergoing elasto-plastic deformation. The additive small strain plasticity model is used [9].

We shall consider the following contact problem: find the generalized stress field $(\sigma, \chi) : \Omega \to R^{d\times d} \times R^{d\times d}$, the displacement field $u : \Omega \to R^d$, the generalized strain field $(\epsilon^p, \xi) : \Omega \to R^{d\times d} \times R^{d\times d}$ satisfying the maximal plastic work principle [9] for generalized stresses as well as

$$\mathrm{div}\sigma + f_1 = 0 \ \text{ in } \ \Omega, \tag{1}$$

$$u = 0 \ \text{ on } \ \Gamma_1 \ \text{ and } \ \sigma_\nu = f_2 \ \text{ on } \ \Gamma_2, \tag{2}$$

$$u_\nu = 0, \ \ | \ \sigma_\tau \ | \leq \mu_f \tilde{p} \ \text{ on } \ \Gamma_3, \tag{3}$$

$$| \ \sigma_\tau \ | \ < \ \ \mu_f \tilde{p} \ \ \Rightarrow \ \ u_\tau = 0 \ \text{ on } \ \Gamma_3, \tag{4}$$

$$\begin{aligned} | \ \sigma_\tau \ | \ = \ \ \mu_f \tilde{p} \ \ \Rightarrow \ \ \exists \lambda \geq 0, \\ u_\tau = -\lambda \sigma_\tau \ \text{ on } \ \Gamma_3. \end{aligned} \tag{5}$$

For the unit outward normal vector ν to the boundary Γ normal and tangential components of the displacement field u are denoted by [9] $u_\nu = u \cdot \nu = u_i \cdot \nu_i$, $i = 1, ..., d$, and by $u_\tau = u - u_\nu \nu$, respectively. Similarly normal and tangential components of the stress field σ are denoted by $\sigma_\nu = \sigma\nu \cdot \nu$ and by $\sigma_\tau = \sigma\nu - \sigma_\nu \nu$, respectively. A real constant $\mu_f > 0$ and $| \cdot |$ denote the friction coefficient and the Euclidean norm, respectively. A real constant $\tilde{p}$ is interpreted as a bound of normal contact stress σ_ν along the boundary Γ_3 [17]. For a given $\tilde{p} \geq 0$ system (1)-(5) governs the elasto–plastic bilateral contact problem with Tresca friction.

Using the regularization as well as penalization techniques [15] the original contact problem (1)-(5) is approximated by the system of coupled nonlinear equations: find $u_\beta \in V$ and $(\sigma_\beta, \chi_\beta) \in S \times S$ satisfying the following system of nonlinear equations for all $(\tau, \eta) \in S \times S$ and $v \in V$,

$$\begin{aligned} \int_\Omega [\sigma_\beta : C^{-1} : (\tau - \sigma_\beta) + \chi_\beta : H^{-1} : (\eta - \chi_\beta)] dx + \\ \tilde{\alpha} \int_\Omega [(\sigma_\beta - P^\alpha_{K_M}(\sigma_\beta)) : (\tau - \sigma_\beta) + (\chi_\beta - P^\alpha_{K_M}(\chi_\beta) : (\eta - \chi_\beta)] dx - \\ \int_\Omega \epsilon(u_\beta) : (\tau - \sigma_\beta) dx = 0, \end{aligned} \tag{6}$$

$$\begin{aligned} \int_\Omega \epsilon(v - u_\beta) : \sigma_\beta(u) dx + \\ \int_{\Gamma_3} \nabla_v j^\rho_c(u_\beta)(v - u_\beta) ds = \\ \int_\Omega f_1(v - u_\beta) dx + \int_{\Gamma_2} f_2(v - u_\beta) ds. \end{aligned} \tag{7}$$

$V \subset H^1(\Omega)$ and $S \subset L^2(\Omega)$ are spaces of admissible displacements and stresses, respectively. For definition of spaces $L^2(\Omega$ and $H^1(\Omega)$ containing square integrable functions and their derivatives, respectively, see [9]. $P^\alpha_{K_M}$ denotes the regularized projection operator of generalized stresses on the set of generalized admissible stresses K_M [15]. Tensors C^{-1} and H^{-1} denote the inverse of compliance and hardening tensor, respectively. Constants $\beta > 0$ and $\tilde{\alpha} > 0$ are regularization parameters [15].

2.2 Optimization problem

Let us formulate the optimization problem for the state system (6)-(7). Let us choose the material density function $\rho = \rho(x)$, $x \in \Omega$, as the design variable. It indicates the solid sub-domain when $\rho \approx 1$ and void sub-domain when $\rho \approx 0$. The objective functional $J(\cdot) : V \to R$ is assumed to depend on the solution $u(\rho)$ to the state system (6)-(7) in the domain Ω. In general this functional is sum of domain and/or boundary integrals, i.e.,

$$\tilde{J}(u(\rho)) = \int_\Omega \psi(u(\rho))dx + \int_\Gamma \tilde{\psi}(u(\rho))ds, \tag{8}$$

where the integrand functions $\psi : R^d \to R$ and $\tilde{\psi} : R^d \to R$ depend also on the solution $u = u(\rho)$ to the state system (6)-(7). These integrand functions are assumed smooth enough and their first derivatives are bounded for every u. The set of admissible material density functions is given by $U_{ad}^{\rho} = \{\rho \in H^1(\Omega) \cap L^\infty(\Omega) : 0 \leq \rho \leq 1, \ \ Vol(\rho) \leq Vol^{giv}\}$. In order to ensure the solvability of the optimization problem we regularize it adding to (8) Ginzburg-Landau free energy functional:

$$E(\rho) = \int_\Omega \psi(\rho)d\Omega, \tag{9}$$

with the integrand function $\psi(\rho) = \frac{\gamma\epsilon}{2} \mid \nabla\rho \mid^2 + \frac{\gamma}{\epsilon}\psi_B(\rho)$. where $\epsilon > 0$ is a constant and constant $\gamma > 0$ is the interfacial energy density parameter. The function $\psi_B(\rho) = \frac{\rho^2}{4}(1-\rho^2)$ is a double-well potential which characterizes the two phases of material [15]. The regularized cost functional $J(\rho, u)$ has the form

$$J(\rho, u) = \tilde{J}(u) + E(\rho), \tag{10}$$

Consider the following topology optimization problem: *find material density function* $\rho^\star \in U_{ad}^{\rho}$ *such that*

$$J(\rho^\star, u^\star) = \min_{\rho \in U_{ad}^{\rho}} J(\rho, u), \tag{11}$$

where $(u(\Omega), \sigma(\Omega), \chi(\Omega))$ is the solution to the state system (6)-(7) in the domain Ω. In applications are considered different cost functionals. Among others, $\psi = 0$, $\tilde{\psi} = \sigma_\nu(u) \cdot \eta_\nu(x)$, $x \in \Omega$, $\eta(x)$ is an auxiliary given bounded function and σ_ν (η_ν) is the normal component of the stress field $\sigma = \sigma(u)$ (η). The other examples include: $\psi = \max\{\sigma, \ x \in \Omega\}$ or $\tilde{\psi} = \sigma_\nu^p, \ p \geq 2$.

2.3 Optimality conditions

Let us use Lagrange multiplier technique to formulate optimality condition for problem (11). Using Lagrangian function for this optimization problem we define the adjoint state $(z, p, q) \in V \times S \times S$ satisfying the system of the adjoint equations for all $v \in V$ and $(\tau, \eta) \in S \times S$:

$$\int_\Omega \frac{d\psi(u)}{du} v dx + \int_\Gamma \frac{d\tilde{\psi}(u)}{du} v ds - \int_\Omega \epsilon(v_\beta) :$$
$$(p - \sigma_\beta) dx + \int_{\Gamma_3} \nabla_v j_c^\rho(v_\beta) z ds = 0, \tag{12}$$

as well as

$$\int_\Omega [\tau_\beta : C^{-1}(p - \tau_\beta) dx + \eta_\beta : H^{-1}(q - \eta_\beta)] dx$$
$$+\tilde{\alpha} \int_\Omega [(\tau_\beta - P'_{K_M}(\tau_\beta)) : p +$$
$$(\eta_\beta - P'_{K_M}(\eta_\beta)) : q] dx +$$
$$\int_\Omega \epsilon(z - u_\beta) : \tau_\beta(u) dx = 0. \tag{13}$$

Using (12)-13) as well as Lagrange multiplier technique we obtain [15] the derivative $J'(\rho)$ of the functional (11) as equal to:

$$J'(\rho) = \int_\Omega \varphi_E(\rho) \eta dx,$$

with $\varphi_E(\rho) = \sigma : (C^{-1})' : p + \lambda : (H^{-1})' : q + \gamma\epsilon \mid \triangle\rho \mid + \frac{\gamma}{\epsilon}\psi'_B(\rho)$. The optimal topology $\rho^\star$ we shall find as the solution to the modified Cahn-Hilliard equation, i.e., gradient flow dynamic equation. Assume ρ is dependent also on artificial time t interpreted as the sequence of computational iterations. Therefore in time interval $[0, T]$, with given $T > 0$, $w = \varphi_E(\rho)$, density function ρ is a solution to [15]:

$$\frac{\partial \rho}{\partial t} = \nabla \cdot (\nabla w) \qquad \text{in } \Omega, \tag{14}$$
$$\nabla w \cdot \nu = \nabla \rho \cdot \nu = 0 \quad \text{on } \partial\Omega, \tag{15}$$
$$\rho(0, x) = \rho_0(x) \qquad \text{in } \Omega,\ t = 0. \tag{16}$$

In the mixed formulation system (14)-(16) for all $(\eta, v) \in H^1(\Omega) \times H^1(\Omega$ takes the form

$$(\partial_t \rho, \eta) + (\nabla w, \nabla \eta) = 0, \tag{17}$$
$$(w, v) = (\nabla \rho, \nabla v) + \frac{1}{\varepsilon^2} b(\rho, \rho, v), \tag{18}$$

where $b(u, v, \eta) = \int_\Omega [\psi'_B(u) \cdot v + \sigma : (C^{-1})' : p + \lambda : (H^{-1})' : q] \eta dx$.

3 Virtual element method

The VEM introduced in [4] is a combination of the standard finite element method (FEM) and the mimetic finite difference method. In order to deal with arbitrarily shaped polygonal elements, VEM uses general finite element spaces that may contain non-polynomial functions. In addition, by avoiding an explicit expression of a basis function and constructing certain operators involved in its discrete problem, the VEM can handle general polygons, including non-convex elements and very distorted elements. However, as for standard FEM, numerical integration is required for the polynomial component and hence we assume that it is possible to compute their contribution by means of some quadrature procedure. One such technique, although by no means the only possibility, is to subdivide each polygon into triangles and use Gaussian integration. However, an appropriate choice of DOFs could drastically decrease explicit numerical integration, as explained later. Due to its firm theoretical foundation [1, 6, 7, 10, 11, 16, 17] and easy implementation, it not only has been extended to nonconforming [6, 7] and discontinuous [18] and mixed [12] VEMs, but also has been applied to solution of many practical problems [18–20].

3.1 Virtual element method for gradient flow equation

We shall use the VEM to discretize and solve the gradient flow equation (17)-(18). For every mesh size h, let $\mathcal{K}_h$ be a sequence of partitions of domain Ω into elements K having diameter h_K and measure $|K|$. This family of partitions is assumed to satisfy standard regularity assumptions [4, 7, 12, 21]. In order to define the lowest discrete virtual element space, we shall define the following H^1 and L^2 polynomial projections of trial functions on the element K. The H^1 projection $\Pi_K^{\bigtriangledown}$: $H^1(K) \to \mathcal{P}_1(K)$ on K for all $v \in H^1(K)$ is defined by:

$$(\nabla \Pi_K^{\bigtriangledown} v, \nabla q)_K = (\nabla v, \nabla q)_K \quad \forall q \in \mathcal{P}_1(K) \tag{19}$$

and on the boundary ∂K $(\nabla \Pi_K^{\bigtriangledown} v, 1)_{\partial K} = (\nabla v, 1)_{\partial K}$. The set $\mathcal{P}_l(K)$ consists from polynomials of degree less than or equal to l on K [4]. The L^2 projection Π_K^0: $L^2(K) \to \mathcal{P}_1(K)$ on K is defined by:

$$(\Pi_K^0 v, q)_K = (v, q)_K \quad \forall q \in \mathcal{P}_1(K), \tag{20}$$

Let us define the local virtual element discrete space on general meshes as

$$\begin{aligned} X_{h|K} = \{ &v_h \in \tilde{X}_{h|K} : \\ &(v_h - \nabla \Pi_K^{\bigtriangledown} v_h, q)_K = 0 \quad \forall q \in \mathcal{P}_1(K) \}, \end{aligned} \tag{21}$$

where the space $\tilde{X}_{h|K}$ is given by:

$$\begin{aligned} \tilde{X}_{h|K} = \{ &v_h \in H^1(K) : \triangle v_h \in \mathcal{P}_1(K), \\ &v_{h|\partial K} \in C^0(\partial K), v_{h|e} \in \mathcal{P}_1(e) \text{ for each } e \in \partial K \}. \end{aligned} \tag{22}$$

As degrees of freedom we can use the values of v_h at the vertices of element K, which matches the dimension of $X_{h|K}$. The global discrete virtual element space has the form:

$$X_h = \{ v_h \in H^1(\Omega) : v_{h|K} \in X_{h|K} \text{ for all } K \in \mathcal{K}_h \}.$$

In order to provide computable discrete approximation of system (17)-(18) we shall use also the following symmetric, positive definite and bilinear forms:

$$S_1^K(\varphi_i, \varphi_j) = \max(1, (\nabla\varphi_i, \nabla\Pi_K^\nabla \varphi_j)_K)\delta_{i,j}, \tag{23}$$

$$S_2^K(\varphi_i, \varphi_j) = \max(\mid K \mid, (\Pi_K^0\varphi_i, \Pi_K^0\varphi_j)_K)\delta_{i,j}, \tag{24}$$

where $\{\varphi_i\}$ denotes the local canonical basis of the space $X_{h|K}$ and $\delta_{i,j}$ is the Kronecker function. Using forms (23)-(24) we can approximate three exact local forms $(\nabla\cdot, \nabla\cdot)_K$, $(\cdot,\cdot)_K$ and $b(\cdot,\cdot,\cdot)_K$ by:

$$\begin{aligned} a_h^K(v_h, \eta_h) = (\nabla\Pi_K^\nabla v_h, \nabla\Pi_K^\nabla \eta_h)_K + \\ S_1^K(v_h - \nabla\Pi_K^\nabla v_h, \eta_h - \nabla\Pi_K^\nabla \eta_h)), \end{aligned} \tag{25}$$

$$\begin{aligned} m_h^K(v_h, \eta_h) = (\Pi_K^0 v_h, \Pi_K^0 \eta_h)_K + \\ S_2^K(v_h - \Pi_K^0 v_h, \eta_h - \Pi_K^0 \eta_h), \end{aligned} \tag{26}$$

$$b_h^K(u_h, v_h, \eta_h) = [|K\mid^{-1} m_h^K(u_h, u_h) - 1]m_h^K(v_h, \eta_h).$$

The first terms of (25) and (26) ensure the consistency of the discrete bilinear forms [4, 12]. The second terms in these forms are called stabilization terms and they guarantee the continuity and coercivity of these forms [4, 12]. Summing up the local forms element by element we obtain the global discrete forms. Since the projections Π_K^∇ and Π_K^0 can be exactly computed only by degrees of freedom therefore the discrete virtual element forms are also computable. Let us assume the partition of the time interval [0, T] with the time step $\tau = T/N$ is uniform and the backward Euler scheme is used to approximate time derivative. For a given $\rho_h^0 \in X_h$ as the virtual Lagrange interpolant of ρ^0 and for all $1 \leq n \leq N$ fully discrete virtual element problem approximating (17)-(18) consists in finding $(\rho_h^n, w_h^n) \in X_h \times X_h$, $1 \leq n \leq N$ such that for all $\eta_h, v_h \in\in X_h \times X_h$ it holds

$$m_h(\frac{\rho_h^n - \rho_h^{n+1}}{\tau}, \eta_h) + a_h(w_h^n, \eta_h) = 0, \tag{27}$$

$$m_h(w_h^n, v_h) = a_h(\rho_h^n, v_h) + \frac{1}{\varepsilon^2} b_h(\rho_h^n, \rho_h^n, v_h). \tag{28}$$

For the convergence result of the scheme (27)-(28) see [7, 11, 12].

4 Numerical example

The first experiment is concerned with testing the convergence of the method for system (17)-(18). The tests have been run on domain $\Omega = [-1, 1]^2$, for $T = 1$, assuming the exact solution $\rho = \sin(\pi x)sin(\pi y)\sin(t)$ either on regular squared mesh (mesh1) or on hexagonal element mesh (mesh2). Tables 1 and 2 present L^2 error results for ρ and w at the end time T. The expected convergence rate with respect to mesh size h is confirmed.

h	$\parallel \rho - \Pi^0_K \rho_h \parallel$	$\parallel w - \Pi^0_K w_h \parallel$
0.12500	$1.4463 \cdot 10^{-2}$	$1.7106 \cdot 10^{-2}$
0.06250	$4.0487 \cdot 10^{-3}$	$5.2561 \cdot 10^{-3}$
0.03125	$1.0398 \cdot 10^{-3}$	$1.6532 \cdot 10^{-3}$

Table 1: Mesh1. L^2 error estimates $\parallel \rho - \Pi^0_K \rho_h \parallel$ and $\parallel w - \Pi^0_K w_h \parallel$ at the time T.

h	$\parallel \rho - \Pi^0_K \rho_h \parallel$	$\parallel w - \Pi^0_K w_h \parallel$
0.12500	$1.9804 \cdot 10^{-1}$	$2.7391 \cdot 10^{-1}$
0.06250	$5.0145 \cdot 10^{-2}$	$7.2554 \cdot 10^{-2}$
0.03125	$1.2354 \cdot 10^{-2}$	$1.5742 \cdot 10^{-2}$

Table 2: Mesh2. L^2 error estimates $\parallel \rho - \Pi^0_K \rho_h \parallel$ and $\parallel w - \Pi^0_K w_h \parallel$ at the time T.

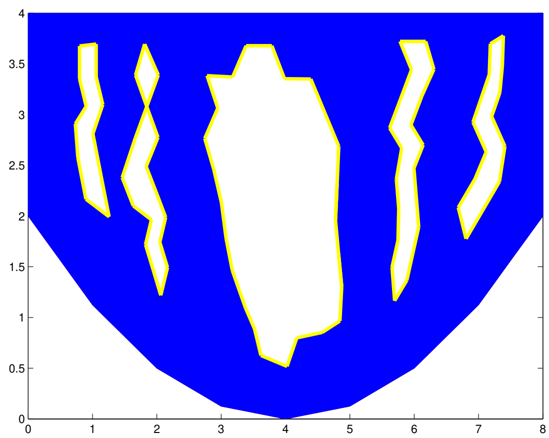

Figure 2: Optimal topology.

The second experiment is concerned with the solution of the topology optimization problem for a body occupying two-dimensional domain $\Omega \subset R^2$ in bilateral contact with the rigid foundation in the Matlab environment. The functional (10) with $\psi(u) = 0$ and $\tilde{\psi}(u) = \sigma(u)\nu$ is chosen as the objective functional. The aim of the topology optimization problem is to reduce the contact stress. The constraint function is equal to volume constraint, i.e., $Vol(\rho) = \int_\Omega dx - V^{giv}$. The domain $\Omega \subset R^2$ is chosen as follows (see Fig. 1)

$$\Omega = \{(x_1, x_2) \in R^2 : 0 \leq x_1 \leq 8 \ \wedge \ 0 < v(x_1) \leq x_2 \leq 4\}, \tag{29}$$

where the function $v(x_1) = 0.125 \cdot (x_1 - 4)^2$ describes the boundary Γ_3. The boundary Γ of the domain Ω is divided into three disjoint pieces: $\Gamma_1 = \{(x_1, x_2) \in R^2 : x_1 = 0, 8 \ \wedge \ 0 < v(x_1) \leq x_2 \leq 4\}$, $\Gamma_2 = \{(x_1, x_2) \in R^2 : 0 \leq x_1 \leq 8 \ \wedge \ x_2 = 4\}$, $\Gamma_3 = \{(x_1, x_2) \in R^2 : 0 \leq x_1 \leq 8 \wedge v(x_1) = x_2\}$.

Domain Ω is filled with the solid material characterized by the Young moduli $E_1 =$

$10 \cdot E_0$ $E_0 = 2.1 \cdot 10^5$ MPa. The Poisson's ratio is equal to $\nu = .3$. The shear and dilation moduli are equal to $8 \cdot 10^4$ MPa and $1,1 \cdot 10^5$ MPa, respectively. The yield stress $\sigma_{tr} = 367,4$ MPa. The hardening parameters are equal to $k_1 = 1 \cdot 10^5$ MPa and $k_2 = 0$ MPa. The body is loaded by the boundary traction $f_2 = -6.5 \cdot 10^7$ N along the boundary Γ_1, the body force $f_1 = 0$ in domain Ω. The hold-all domain D is a rectangle $[0, 8] \times [0, 4]$. This domain is divided into hexagonal grid with $h = 1/16$. Fig. 2 displays the obtained optimal topology. The areas of weak material appear in the central part of the domain Ω and close to the clamped boundary Γ_2. The mass of the optimal structure is larger for elasto-plastic material in comparing to elastic material model. The algorithm tries to avoid the generation of plastic zones which are less rigid and induce larger displacements. Von Mises effective stress concentration areas appear close and above the contact zone.

Remark VEM does not require explicit computation of the shape functions and their gradients. It implies it is less sensitive to degenerated polyhedra as compared to the standard FEM. In terms of optimization problems, VEM offers the great flexibility in element geometries and local space definitions. Therefore the proposed VEM-based topology optimization is capable to produce designs with improved geometrical resolution as compared to the standard topology optimization framework with element-wise constant design variables and material densities. For a given mesh, because the size of the stiffness matrix is identical for FEM and VEM frameworks, the proposed VEM framework is able to consider a significantly bigger number of design variables than the standard one with almost identical computational effort. It allows to achieve a higher efficiency. The proposed framework is flexible in imposing various pattern and layout constraints and can lead to designs that are directly manufacturable by 3D printing.

5 Conclusions

The obtained results indicate that presented approach based on the application of the Virtual Element Method can be used to solve numerically a topology optimization problem for bodies in bilateral frictional contact. Nonlinear small strain elasto-plastic with linear kinematic hardening material model rather than elastic material model is used. VEM allows to improve the verification of contact conditions and is suitable for complex geometries domains. VEM based approach, by exploiting the advantages of polyhedral elements, offers an effective tool for mesh adaptation in topology optimization. It is capable of finding topologies that generates minimum contact stress. This approach is flexible and can be extended to solve other topology optimization problems for structures governed by other nonlinear equations. The use of higher order VEM especially for non-smooth problems will be subject of future research.

References

[1] D. Adak, G. Manzini, and S. Natarajan. Virtual element approximation of two-dimensional parabolic variational inequalities. *Computers and Mathematics with Applications*, 116:48–70, 2022.

[2] S. Adly, L. Bourdin, F. Caubet, and A.J. de Cordemoy. Shape optimization for variational inequalities: The scalar tresca friction problem. *SIAM Journal on Optimization*, 33(4):2512–2541, 2023.

[3] P.F. Antonietti, M. Bruggi, S. Scacchi, and M. Verani. On the virtual element method for topology optimization on polygonal meshes: A numerical study. *Computers & Mathematics with Applications*, 74(5):1091–1109, 2017.

[4] L. Beirão da Veiga and et al. Basic principles of virtual element methods. *Mathematical Models and Methods in Applied Sciences*, 23(1):99–214, 2013.

[5] H. Chi, A. Pereira, I.F.M. Menezes, and G.H. Paulino. Virtual element method (vem)-based topology optimization: an integrated framework. *Structural and Multidisciplinary Optimization*, 62:1089–1114, 2020.

[6] M. Cihan, B. Hudobivnik, J. Korelc, and P. Wriggers. A virtual element method for 3d contact problems with non-conforming meshes. *Comput. Methods Appl. Mech. Engrg.*, 402:115385, 2022.

[7] A. Dedner and A. Hodson. A higher order nonconforming virtual element method for the cahn hilliard equation. *J. Sci. Comput.*, 101:81, 2024.

[8] C. Hager and B.I. Wohlmuth. Nonlinear complementarity functions for plasticity problems with frictional contact. *Comput. Methods Appl. Mech. Engrg.*, 198:3411–3427, 2009.

[9] W. Han and B.D. Reddy. *Plasticity. Mathematical Theory and Numerical Analysis*. Springer, New York, 2013.

[10] J. Huang and Y. Yu. Some estimates for virtual element methods in three dimensions. *Comput. Methods Appl. Math.*, 23(1):177–187, 2023.

[11] W. Liu, Y. Chen, and Q. Liang. Unified analysis of conforming and nonconforming virtual element methods for nonlinear sobolev equations. *Calcolo*, 62:7, 2025.

[12] X. Liu and Z. Chen. A virtual element method for the cahn hilliard problem in mixed form. *Applied Mathematics Letters*, 87:115–124, 2019.

[13] M. Mengolinia, M.F. Benedetto, and A. M. Aragóna. An engineering perspective to the virtual element method and its interplay with the standard finite element method. *Comput. Methods Appl. Mech. Engrg.*, 350:995–1023, 2019.

[14] A. Myśliński. Phase field topology optimization of elasto-plastic contact problems with friction. In A. Zignoni, editor, *Current Perspectives and New Directions in Mechanics, Modelling and Design of Structural Systems*, pages 464–470. CRC Press, Taylor & Francis, London, 2022.

[15] A. Myśliński. Phase field approach to topology optimization of elasto-plastic contact problems. In S. Migórski and M. Sofonea, editors, *Nonsmooth Problems with Application in Mechanics*, volume 127, pages 167–189. Banach Center Publications, 2024.

[16] G. Pradhan and B. Deka. Optimal convergence analysis of the virtual element methods for second-order sobolev equations with variable coefficients on polygonal meshes. *J. Appl. Math. Comput.*, 70:2313–2341, 2024.

[17] F. Wang and B.D. Reddy. A priori error analysis of virtual element method for contact problem. *Fixed Point Theory and Algorithms for Sci. Eng.*, 10:1–12, 2022.

[18] P. Wriggers, F. Aldakheel, and B. Hudobivnik. Virtual element methods for engineering applications. In P.F. Antonietti, L. Beirão da Veiga, and G. Manzini, editors, *The Virtual Element Method and its Applications*, pages 557–605. Springer, Cham, 2022.

[19] P. Wriggers, F. Aldakheel, and B. Hudobivnik. *Virtual Element Methods in Engineering Sciences*. Springer, 2024.

[20] P. Wriggers, W.T. Rust, and B.D. Reddy. A virtual element method for contact. *Comput. Mech.*, 58:1039–1050, 2016.

[21] B.B. Xu, W.F. Fan, and P. Wriggers. High-order 3d virtual element method for linear and nonlinear elasticity. *Computer Methods in Applied Mechanics and Engineering*, 431:117258, 2024.